Preprint Title Oxidation of nanocrystalline silicon at room temperature and various humidity

Authors Vadim M. Popelensky, Sergey G. Dorofeev, Nikolay N. Kononov, Sergey S. Bubenov and Alexander A. Vinokurov

Publication Date 15 Okt 2019

Article Type Full Research Paper

ORCID® iDs Vadim M. Popelensky - https://orcid.org/0000-0002-0994-6455;
Sergey S. Bubenov - https://orcid.org/0000-0002-3022-4326;
Alexander A. Vinokurov - https://orcid.org/0000-0003-1087-9023

Oxidation of nanocrystalline silicon at room temperature and various humidity

Vadim M. Popelensky[1], Sergey G. Dorofeev[1*], Nikolay N. Kononov[2], Sergey S. Bubenov[1], Alexander A. Vinokurov[1]

1. Department of Chemistry, Lomonosov Moscow State University, 1-3 Leninskie Gory, Moscow 119991, Russia

2. Prokhorov General Physics Institute, Russian Academy of Sciences, 38 Vavilov Str., Moscow 119991, Russia

Email:

Sergey G. Dorofeev* – dorofeev_sg@mail.ru

* - Corresponding author

Abstract

Oxidation of HF vapor-etched nanocrystalline silicon films, prepared by drop coating from nanocrystalline Si sol in acetonitrile, was studied. Oxidation of nc-Si at room temperature in air with 5% and 86% relative humidity was observed by means of IR spectroscopy for 2 days. The change in film mass after 15 hours of oxidation was determined using quartz crystal microbalance. In dry air, film mass and integral intensity of bands attributed to vibrations in Si_{3-x}–Si–H_x and Si-O-Si groups changed linearly with time. In humid air, intensity of in Si_{3-x}–Si–H_x band decays exponentially and intensity of Si-O-Si band increases as a square root of oxidation time. Film mass gain after 15 hours of oxidation corresponds to an average oxide layer thickness of 0.02 nm in dry air and 0.51 nm in wet air.

Keywords: etching; IR spectroscopy; silicon nanocrystals; oxidation; quartz microbalance;

Introduction

Nanocrystalline silicon (nc-Si) has been studied extensively for the last few years due to the possibility to use it for the production of optical [1], light emitting [2] and electronic [3,4] devices and biosensors [5]. Silicon dioxide that is formed on the surface of silicon nanocrystals is of great importance for some other applications such as fabrication of integrated circuits.

The first studies of silicon oxidation were devoted to the thermal oxidation of monocrystalline Si [6-9], but with a decrease of the used integrated circuits' size the process of unprompted oxide growth on Si surface exposed to air at room temperature became more important. According to these studies, the thickness of native oxide does not exceed the size of 0.1 nm, but it has been experimentally proven [10] that after 10 hours of air exposure at room temperature the oxide layer of 1.0-1.2 nm is achieved. Therefore, it is likely that the oxidation of Si at room temperature follows a different mechanism from the one assigned to the thermal oxidation process. The oxidation of monocrystalline Si in dry oxygen, air and ultrapure water was studied in [11, 12]. These works revealed that the oxide thickness increases over time as a step-like function and that an efficient growth of oxide requires both water and oxygen. The rate of oxidation can be reduced by lowering the content of moisture in the air and oxygen in ultrapure water.

The properties of nc-Si are very different from the ones of monocrystalline Si [13]: the coexistence of a large number of different crystallographic planes on the surface of silicon nanoparticles, surface curvature and the amorphization of near-surface Si layers during the oxidation must result in a difference between oxidation kinetics for mono- and nanocrystalline silicon. Moreover, nc-Si has a much higher surface to volume ratio, which means that the effect of the surface oxide layer on the nc-Si properties is much greater in comparison with a monocrystalline Si. The oxidation of nc-Si can readily take place in air even at room temperature [11]. This may make it difficult to produce an oxide film of given thickness, especially for nanometer-scale films. Therefore, for the proper use of nc-Si we must study the process of its oxidation in air at room temperature.

As of now, several studies about the oxidation of nc-Si have already been conducted. These works feature different ambient conditions and methods of pre-oxidation treatment. Usually nc-Si are etched in HF to clean it from the initial oxide with acid- and vapor- etching both being used. The change in oxide stoichiometry before etching and after etching and oxidation was reported in [14], with initial oxide being the stoichiometric one and the new one appearing to be a suboxide $SiO_{1.95}$. Silicon to oxygen ratio was acquired from the Si-O-Si stretching vibration frequency shift in infrared (IR) spectra, according to the dependence from [15]. The change of oxygen content is attributed to the reconstruction of silicon surface after the removal of hydrogen from the surface of the etched nanoparticles [16]. The decrease in photoluminescence (PL) intensity after etching and oxidation was caused by an increase in the number of defects in nc-Si, which is confirmed by the electronic spin resonance (ESR) method. It was also shown that the size of nanoparticles decreased based on PL data. Aside from simple HF etching, etching with following vacuum annealing or hydrosilylation with 1-octadecene was investigated by the means of IR spectroscopy [17]. After HF etching Si-O-Si band disappears and Si-H appears. During oxidation the former line returns and the latter one decays, while another Si-H band with higher frequency appears and its intensity rises over time. Annealing has no effect on oxidation, but hydrosilated nc-Si are more resistant to oxidation. It was demonstrated that oxidation of nc-Si does not proceed in dry air or degassed water at room temperature [18], but the addition of moisture or oxygen respectively activates the process. Similar results were achieved for monocrystalline Si [11]. The use of oxidizing agents' solutions ($KMnO_4$, H_2SO_4/H_2O, $K_2S_2O_8$) was researched, but the correlation between the red-ox potential and oxidation rate could not be established. The use of any of these oxidizing agents led to the complete removal of Si-H bonds from the surface of nc-Si [19]. The results obtained in reviewed works on nanosilicon oxidation do not contain data on the thickness of the oxide layer formed during the oxidation of nc-Si.

In this work, we studied the process of nc-Si oxidation in air at room temperature with varied humidity using IR spectroscopy and direct measurement of film mass. The latter was performed on quartz crystal resonators on which the film was deposited. Using the obtained data, we calculated the native oxide growth rate.

Results and discussion

IR-spectra evolution during the oxidation of nc-Si

IR transmittance spectra of nc-Si films deposited on silver substrate upon etching and oxidation are present on figure 2. Spectra (1) on the left are taken at 5% relative humidity (RH), and (2) on the right – at 86% RH. In both cases (a)-spectrum corresponds to the initial non-etched nc-Si films and is characterized by pronounced absorption band at 1240-940 cm^{-1} that conforms to various vibrational mods of Si-O-Si bonds [20]. This band almost completely disappears after 15 minutes of etching with HF vapors and 3 minutes of vacuum drying (figure 2, (b)-spectrum), but Si-H band at 2165-2050 cm^{-1} emerges. Spectra (c) and (d) on figure 2, which were taken for samples that were oxidized for 20 and 50 hours respectively, show that integral intensity (further, intensity) of this Si-H band decreases upon oxidation (figure 3). At the same time for the case of high humidity another Si-H band at 2285-2185 cm^{-1} appears and its intensity increases (figure 4). The same Si-H band presents on IR spectrum of the initial non-etched film. The fact that this band does not appear upon oxidation in dry air witness that water affects the nc-Si films oxidation process. According to literature [21] the band at 2285-2185 cm^{-1} corresponds to Si-H vibrations in O_ySi_x-Si-H_{4-y-x} group in which silicon atom is bind to oxygen atom whereas the band at 2165-2050 cm^{-1} corresponds to Si-H vibrations in H_{4-x}–Si–H_x unoxidized group. The initial intensity for this Si-H band in both cases of RH does not depend on humidity because silicon nanoparticles are equally and completely covered with Si-H bonds after etching. Therefore, the intensities of Si-H and Si-O-Si bands on figures 3 - 5 were normalized by initial Si-H band intensity.

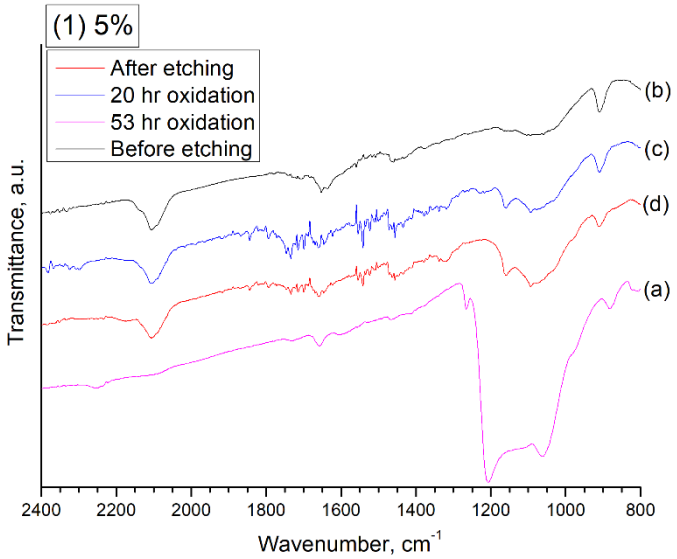

Figure 1 (1). IR-spectrum of nc-Si before (a) and after (b) etching in HF vapor and after 20 (c) and 50 (d) hours of oxidation at 5% relative humidity.

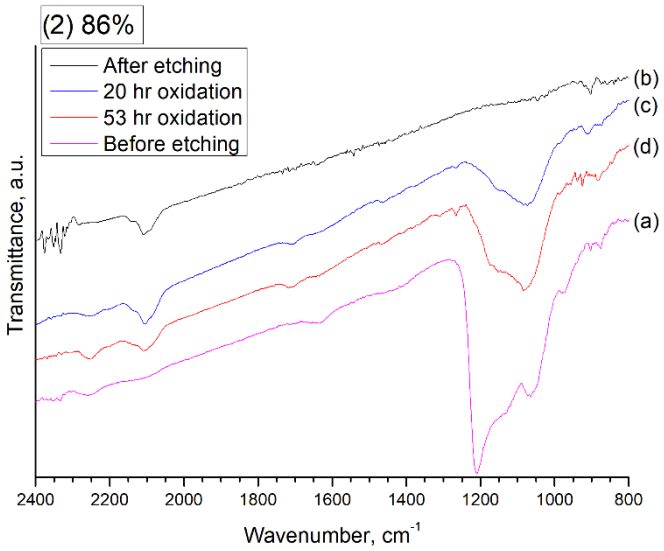

Figure 1 (2). IR-spectrum of nc-Si before (a) and after (b) etching in HF vapor and after 20 (c) and 50 (d) hours of oxidation at 86% relative humidity.

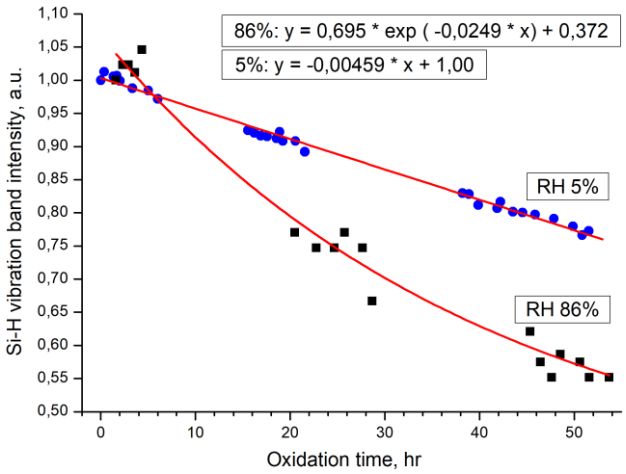

Figure 2. Integral intensities of 2165-2050 cm^{-1} Si-H band over oxidation time for 5% and 86% relative humidity. Equations for fitting curves for both relative humidities (RH) are given.

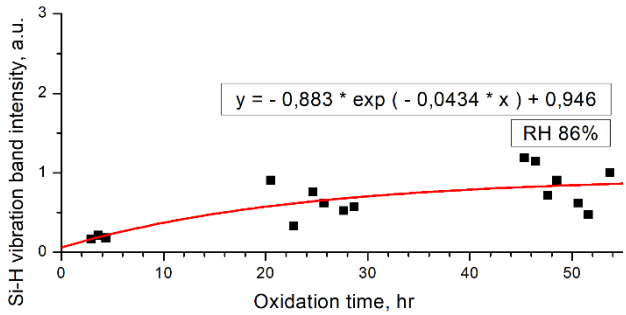

Figure 3. Integral intensities of 2285-2185 cm^{-1} Si-H band over oxidation time for 86% relative humidity. Equation for fitting curve is given.

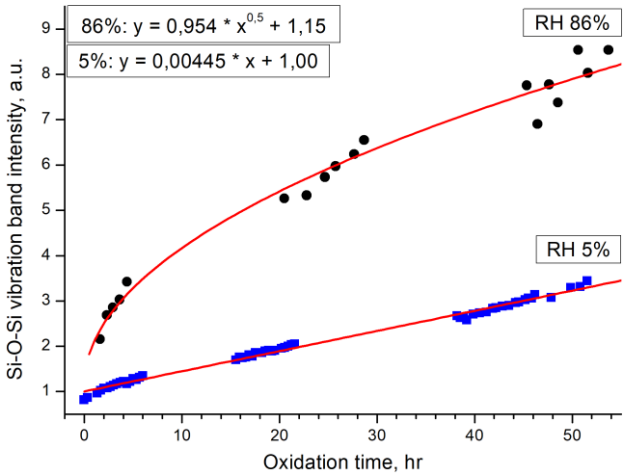

Figure 4. Integral intensities of 1240-940 cm^{-1} Si-O-Si band over oxidation time for 5% and 86% relative humidity. Equations for fitting curves for both relative humidities (RH) are given.

Integral intensities of Si-O-Si bands throughout oxidation for 5 and 86% RH are given on figure 5 and are proportional to quantity of oxidized silicon in the samples. In case of high humidity, the quantity of oxidized silicon rises faster than in the case of dry air. As it can be seen from figure 3 the Si-H band at 2165-2050 cm^{-1} decreases faster in wet air than in dry air. It can be concluded that the rate of nanosilicon oxidation is higher in wet air than in dry and that Si-H bonds change to Si-O-Si ones upon oxidation.

Oxidation of nanosilicon films at high humidity (see figure 5) is in good agreement with Deal-Grove model, in which the thickness of oxidized layer is proportional to square root of oxidation time. The process consists of a fast initial oxidation stage and the following slower stage, which confirms the molecular dynamics calculations [22] and other experimental data [17]. Oxidation in dry air goes much slower and can be fitted with linear function. There are constant terms in polynomial fits on figure 5 that indicate the presence of traces of initial silicon oxide in etched nc-Si films. Oxidation could take place during evacuation in the process of removal of HF vapors after etching. Maximum of Si-O-Si band is sensitive to the stoichiometry of forming silicon oxide [15]. It was established that at 86% RH the maximum is at 1074 cm^{-1} and stoichiometric oxide SiO_2 is formed, whereas at 5% RH maximum shifts to 1069 cm^{-1} what corresponds to nonstoichiometric $SiO_{1.95}$.

Mass change upon oxidation

Mass change upon oxidation of nanosilicon films was studied by the means of quartz microbalances. The results are given on figure 6, initial masses of films are normalized to 1. IR-spectroscopy (see above) demonstrates that the quantity of silicon oxide in nc-Si films just after the etching is low and the mass of hydrogen on the nanoparticles' surface is approximately 0.3%

of film weight so it could be presumed that only the silicon determines the initial mass of nanosilicon film after etching. As can be seen in figure 6 at low RH the mass change is very low (0.7%) whereas for the case of 86% RH it rises by 38% in 15 hours. At very high humidity water can be adsorbed by the surface of silicon nanoparticles so this film was purged with dry air for 25 hours to dispose of adsorbed water molecules. In 1 hour of such treatment the film mass decreased to 124% of initial value and changes almost stopped. The final relative mass change upon 15 hours of oxidation are 0.7 and 24% for 5 and 86% RH.

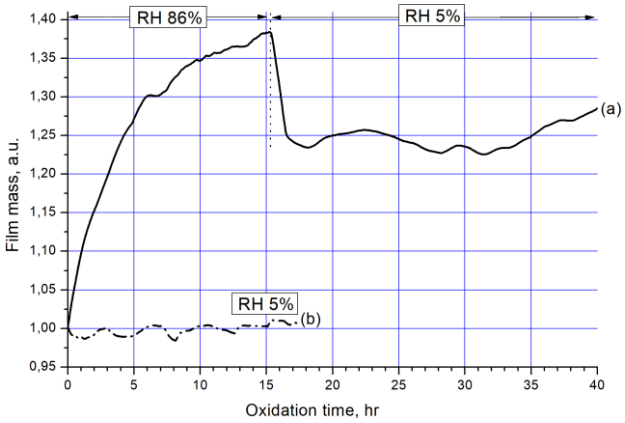

Figure 5. Mass change of nc-Si films over oxidation time at high (a) and low (b) relative humidity. Initial masses of films are normalized to 1. To remove adsorbed water and calculate the mass of nc-Si and its oxide, sample in (a) was purged with dry air, which is indicated by the change of RH. Dotted vertical line denotes the beginning of purging.

TEM image of etched nc-Si particles is given in figure 7 and their size distribution histogram is present in figure 8. Mean particle diameter is 12.9 nm. Assuming that silicon nanoparticles in the films are spherical both before oxidation and after as well as taking into account the mean particle diameter after etching, their relative mass change upon oxidation, and density of silicon and amorphous silica (2.329 and 2.196 g/cm^3, respectively) the thickness of oxide layer was estimated. After 15 hours of oxidation the thickness of amorphous SiO_2 is 0.02 and 0.51 nm for 5 and 86% RH and the oxidation speed is approximately 0.001 and 0.034 nm/hr, respectively. Oxidation speed

for the low humidity coincides with one obtained for monocrystallic silicon [11] in the same experimental conditions. We could not compare our results of nanosilicon oxidation with data on monocrystallic silicon oxidation in wet air because authors of [11] did at it at 42% RH.

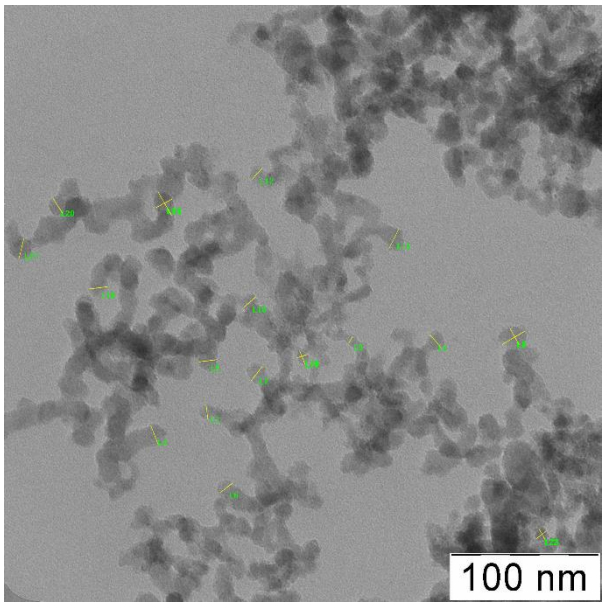

Figure 6. TEM image of etched silicon nanoparticles. Yellow lines are some of the measurements of particles' size.

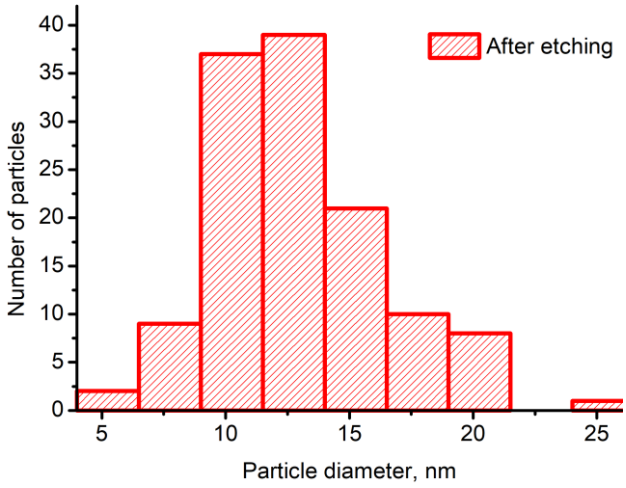

Figure 7. Distribution of etched particles' diameter.

Conclusion

Oxidation of HF vapor-etched nanocrystalline silicon films, prepared by drop coating from nc-Si sol in acetonitrile, was studied. Oxidation of nc-Si at room temperature in air with 5% and 86% relative humidity was observed by means of IR spectroscopy for 2 days. The change in film mass after 15 hours of oxidation was determined using quartz crystal microbalance. In dry air, film mass and integral intensity of bands attributed to vibrations in Si_{3-x}–Si–H_x and Si-O-Si groups changed linearly with time. In humid air, intensity of in Si_{3-x}–Si–H_x band decays exponentially and intensity of Si-O-Si band increases as a square root of oxidation time. Band, attributed to the Si-H vibrations in O_ySi_x–Si–H_{4-x-y} group, was detected during oxidation in humid air only and its intensity increased throughout oxidation process. Film mass gain after 15 hours of oxidation corresponds to an average oxide layer thickness of 0.02 nm in dry air and 0.51 nm in wet air.

Experimental section

Silicon nanoparticles were synthesized by laser-induced pyrolysis of gaseous monosilane [23]. Nanoparticles were dispersed in acetonitrile, the the resulting sol had concentration of 3-5 mg/ml. Sol was dripped onto quartz resonators (frequency 12 MHz) in the area of one of the silver electrodes. Another blank quartz resonator was used as a comparison sample to take into account the side processes such as etching and ageing of quartz crystals and others. Both of the resonators were opened simultaneously so that the ageing processes were equal. After the deposition of nc-Si film both quartz resonators were exposed to HF vapors for 15 minutes to remove the oxidized layer of silicon, vaccum dried for 3 minutes in order to remove the traces of TF and then placed into experimental chamber with regulated humidity (see figure 1). The chamber was constantly purged by air with exact humidity: 5 and 86% for first and second sample respectively. The humidity was regulated by mixture of two air flows: the first one was dried by zeolite (3 Å, heated at 300 °C for 3 hours), the other one was sparged through the water. The humidity was controlled by Honeywell HIH-4000 sensor.

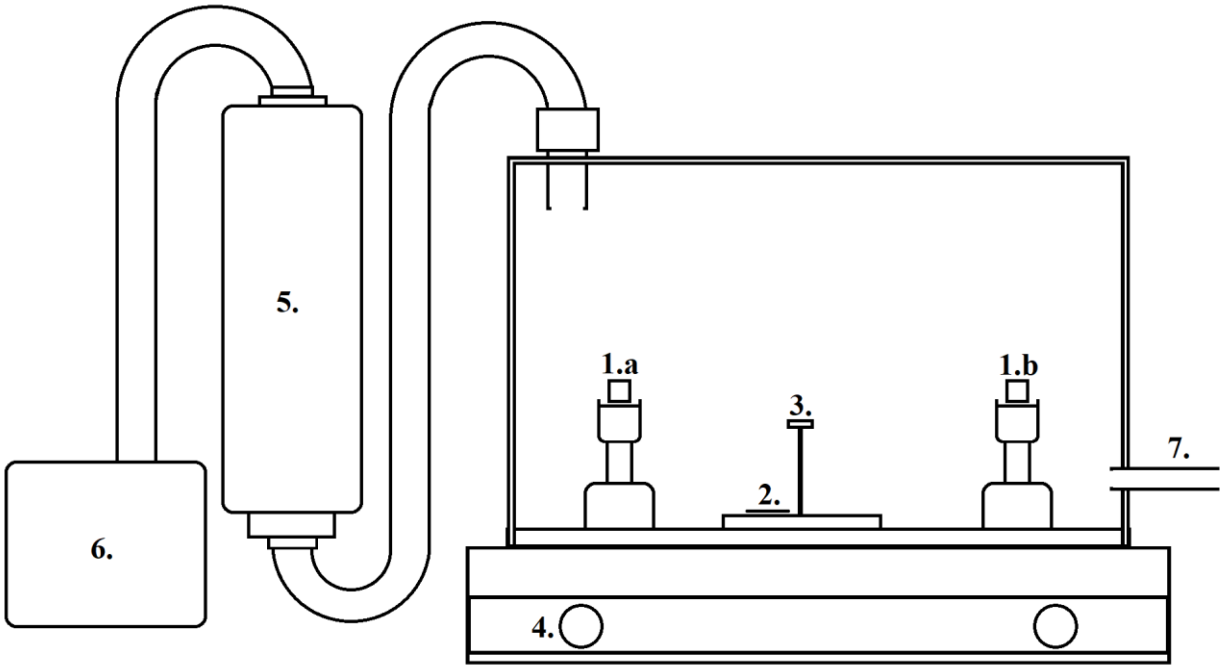

Figure 8: The scheme of experimental device for nc-Si films oxidation studies. 1.a-b – quartz crystals with nc-Si films, 2 – silver substrate with nc-Si film for IR studies, 3 – humidity sensor, 4 – electrical joints, 5 – desiccant with zeolite, 6 – compressor, 7 – air exhaust.

Samples for IR studies were obtained by dripping nc-Si sol onto silver substrates and treated the same way as the ones on the quartz resonators. IR-spectra were taken after certain periods of time on Perkin-Elmer Frontier FTIR-spectrometer with Pike diffusion reflection module, blank silver substrate was used as baseline. All IR spectra were taken from the same area of nc-Si film. Si-O-Si and Si-H bands were integrated for quantitative analysis.

Relative mass change measurements of nanosilicon films upon oxidation were done on quartz crystal microbalances that worked on resonance principle. Resonant frequency measurements were performed as follows. Both resonators – with nanosilicon film and without one – were connected to two identical generators assembled according to the Kolpitz scheme, their resonant frequency was measured by two frequency meters (SANJAN STUDIO PLJ-8LED-RS) that were connected to computer by microcontroller made by I.Makeev. The resonant frequency-time

dependence for nc-Si film was plotted and then the resonant frequency shift of the blank sample was subtracted. The resulting dependence was attributed only to the mass change of nanosilicon layer.

Transmission electron microscopy (TEM) was performed on a LEO912 AB OMEGA microscope (acceleration voltage: 200 kV, resolution: 0.37 nm). Size distributions of etched nanoparticles were obtained through manual calculations of nc-Si images.

Acknowledgements

This work was supported by Russian Foundation for Basic Research grant No 17-03-01269. The authors acknowledge (partial) support from M. V. Lomonosov Moscow State University Program of Development.

References

1. Kanemitsu, Y. *Phys. Rep.* 1995, 263, No. 1.

2. Gaburroa, Z.; Puckera, G.; Belluttib, P; Pavesi, L. *Solid State Commun.* 2000, 114, No. 1.

3. Ostraat, M. L.; De Blauwe, J. W.; Green, M. L.; Bell, L. D.; Brongersma, M. L.; Casperson, J.; Flagan, R. C.; Atwater, H. A. *Appl. Phys. Lett.* 2001, 79, No. 3.

4. Conibeer, G.; Green, M.; Corkish, R.; Cho, Y.; Cho, E.; Jiang, C.; Fangsuwannarak, T.; Pink, E.; Huang, Y.; Puzzer, T.; Trupke, T.; Richards, B.; Shalav, A.; Lin, K. *Thin Solid Films.* 2006, 511, 654-662.

5. Ji, X.; Wang, H.; Song, B.; Chu, B.; He, Y. *Front Chem.* 2018, 6, No. 38.

6. Grove, A. S.; Deal, B. E.; Snow, E. H.; Sah, C. T. *Solid-State Electron.* 1965, 8, 145-163.

7. Hess, D. W.; Deal, B. E. *J. Electrochem. Soc.* 1977, 124, No. 5.

8. Massoud, H. Z.; Plummer J. D. *J. Appl. Phys*. 1987, 62, No. 8.

9. Massoud, H. Z.; Plummer J. D. *J. Electrochem. Soc.* 1985, 132, No. 11.

10. Raider, S. I.; Flitsch, R; Palmer, M. J. *J. Electrochem. Soc*. 1975, 122, No. 3.

11. Morita, M.; Ohmi, T.; Hasegawa. E.; Kawakami, M.; Ohwada, M. *J. Appl. Phys*. 1990, 68, No. 3.

12. Niwano, M.; Kageyama, J.; Kurita K. *J. Appl. Phys*. 1994, 76, No. 4.

13. Koshida, N.; Matsumoto, N. *Mater. Sci. Eng. R Rep*. 2003, 40, No. 5.

14. Pi, X. D.; Mangolini, L.; Campbell, S. A.; Kortshagen, U. *Physical Review B.* 2007, 75, No. 8.

15. Pai, P. G.; Chao, S. S.; Takagi, Y.; Lucovsky, G. *J. Vac. Sci. Technol.* 1986, 4, No. 3.

16. Yu, D. K.; Zhang, R. Q.; Lee, S. T. *J. Appl. Phys*. 2002, 92, No. 12.

17. Niesar, S.; Pereira, R. N.; Stegner, A. R.; Erhard, N.; Hoeb, M.; Baumer, A.; Wiggers, H.; Brandt, M. S.; Stutzmann, M. *Adv. Funct. Mater*. 2012, 22, 1190–1198.

18. Sprung, C.; Heimfarth, J.; Erler, J.; Ziegenbalg, G.; Patzold, C.; Singliar, U.; Frohlich, P.; Muller, A.; Schubert, C.; Roewer, G.; Bohmhammel, K.; Mertens, F.; Seidel, J.; Bertau, M.; Kroke, M. *Silicon*. 2015, 7, No. 1.

19. Litvinenko, S.; Alekseev, S.; Lysenko, V.; Venturello, A.; Geobaldo, F.; Gulina, L.; Kuznetsov, G.; Tolstoy, V.; Skryshevsky, V.; Garrone, E.; Barbier, D. *Int. J. Hydrog. Energy*. 2010, 35, No. 13.

20. Weldon, M. K.; Queeney, K. T.; Gurevich, A. B.; Chabal, Y. J.; Raghavachari, K. *J. Chem. Phys*. 2000, 113, No 6.

21. Falcao, B. P.; Leitao, J. P.; Soares, M. R.; Ricardo, L.; Aguas, H.; Martins, R.; Pereira, R. N. *Phys. Rev. Appl*. 2019, 11, No. 2.

22. Khalilov, U.; Neyts, E. C.; Pourtois, G.; van Duin, A. C. T. *J. Phys. Chem. C*. 2011, 115, 24839–24848.

23. Kuz'min, G. P.; Kononov, N. N.; Rozhanskii, N. V.; Surkov, A. A.; Tikhonevich, O.V. *Mater. Lett.* 2012, 68, 504-506.